Chapter 3

Physiology in phylogeny: Modeling of mechanical driving forces in cardiac development

3.1 Introduction

In pursuing the evolutionary history, or phylogeny, of the heart we look for common characteristics between the embryonic and adult hearts. One pronounced similarity is in the helical organization of the muscle fibers. The simple helical organization of the fibers has long been observed histologically [20]. Moreover, there is some evidence that the muscle fibers, unlike the collection of fibers that includes collagen, are in a double helical bundle. This has been observed in a controversial illustration where the collagen is removed from the heart by boiling [21, 59]. While the idea that such a band exists was formed on the basis of disputed histological evidence, in recent DTMRI studies done by Helm et al. one can easily identify the band architecture (figure 3.1) [23]. This is significant, because this method images the actin, which is present in muscle fibers, but not in the collagen matrix or any other part of heart tissue.

By Ernst Haeckel's premise that ontogeny follows phylogeny, researchers use embryonic fish heart as a biological model for the human embryonic heart [5, 6]. By keeping track of the fluorescent myocardial cells, it is possible to create a picture of their movement during a heart beat. The resulting looped movement is not symmetric, forming an oval for each cell. The long axis of these ovals has to be aligned with the direction of the fiber, since that is the major direction of the contraction. The directionality of the oval paths of the myocardial cells is not constant throughout the heart tube. The only way, that a muscle fiber could have such a non-constant direction as seen in the images is if it was helically arranged [7, 8]. These fibers are not only helically shaped but they seem to be bundled into a band. Thus, both the adult heart and the embryonic heart seem to be comprised of helical muscle bands. How are these two observations related?

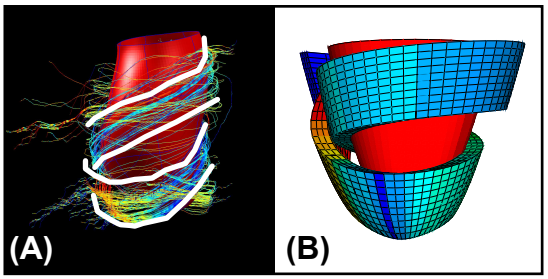

Figure 3.1: Images of the muscle fibers in the heart contrasted with the band model. (A) DENSE MRI image of the muscle fibers in the myocardium given to us by Helm. The muscle fibers are color coded for the value of the pitch angle; blue - horizontal to red - vertical. The red structure in the middle indicates the endocardial surface and represents the left ventricle volume. We overlay white lines on the image to indicate where the band lies. The muscle fibers are more horizontal at the top band section, while at the left section of the bottom band they are more vertical and are accordingly colored yellow and red. (B) The double helix model, color coded in the same manner as the DTMRI images. Blue for horizontal pitch angles to red for vertical pitch angles. The model band repeats the same pattern as the muscle fibers in the DTMRI images - the top portion of the band is dominantly horizontal, while the left section of the bottom portion of the band is going sharply up. The red structure inside the band is the modeled left ventricular volume.

3.1.1 Some Hints from Embryonic Heart Development

In the embryo, the heart muscle fibers start as a simple spiral, but as the embryo develops, the fibers transform into a more complex double helical structure. It would be interesting to track how this development occurs, and how it is reflected in the fiber arrangement of the adult heart.

In general we can imagine a transformation, intriguing in its simplicity, which can be performed on the helix of the embryonic heart converting it to the double helix shape of the adult heart. This transformation is easy to perform on a ribbon (figure 3.2). Of course, there is a world of difference between deforming ribbons and the actual heart muscle. So how does nature achieve this transformation?

3.1.1.1 The development of the heart

The embryonic heart in the beginning stages of its development is a tube with two sulcus [4]. In humans, it starts beating on the twenty second day after conception, and soon thereafter it starts to loop. The driving mechanism for this change of shape has not been fully established. The heart tube goes through a sequence of bending and twisting, first going into an “c” loop, then an “s” loop that is “matured,” after which the main architecture of the four chamber heart is discernible [11, 60]. By the eighth week some of the chamber walls are remodeled and the heart takes on the form of the four chamber pump.

This looping has been experimentally modeled using an elastic tube [12]. It was observed, that the tube upon increasing twist deforms in the same way as the heart tube seen in direct images

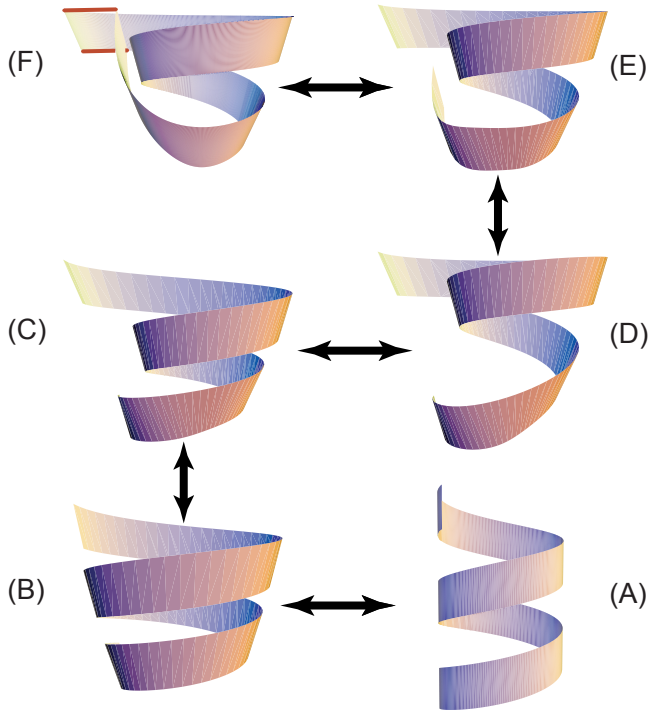

Figure 3.2: A possible set of steps in the development from a spiral tube to a double helix band. (A) A spiral wound around a tube like in an embryonic model. (B) A spiral wound around a tube, that has a varying diameter. (C) The diameter of the tube changes such that the bottom and top loops of the spiral have a larger diameter than the middle loop. (D) The pitch angle of the bottom part of the band is changed to be more vertical. (E) The end of the spiral band is brought up toward the top end. (F) Both ends of the band are at the same level and can be connected to each other; This shape is the same as the double helix proposed by Torrent-Guasp as a heart model.

from chick embryos. Most importantly, the shape of the tube evolves in the same manner as the transformation of ribbon depicted in figure 3.2. However, the mechanical experiment of paper [12] starts at the "c" loop stage and explores the mode of rotation of the looping heart, not the driving forces necessary for such a deformation. Neither do these authors investigate the causes of the twist necessary to induce this transformation. Nevertheless, this experiment strongly suggests that the shape change is governed by elastic mechanical properties of the material rather than a specific genetically encoded biological mechanism.

3.1.1.2 A basic observation

In support of the hypothesis of the dominant role of the mechanics in the heart's transformation, let us consider a simple tactile experiment. Take a rubber tube, such that your thumbs fit snugly at the ends, insert your fingers into the tube and twist it – you can feel the stress on your fingers. Now, without untwisting, deform the tube to relieve the stress. It is remarkable how similar the resulting shape is to the "c" shape of the developing heart. This type of deformation is a well

known phenomenon in solid mechanics, where the structure bends to relieve stress caused by twist. Additionally, it is common in nature for stresses to play an important role in biological growth and development, for example in the growth of tree branches [61]. From these arguments we hypothesize that the stress from the twist causes the deformation in the embryonic heart. However, in our tactile experiment, we first needed to rotate our fingers to produce any change. So, what happens in the heart tube to induce the twist in the first place? In this light, it is curious that the heart begins to loop almost immediately after it starts beating. This is intriguing, since the contraction of the heart muscle is the only source of the force on the tube, not present before the looping was initiated. Thus we will look for the causes of the twist in the tube's response to the muscle fiber contractions.

H.R. Crane once wrote on the general problems of biological growth. He pointed out, that while the process in the whole can be too complex for us to produce an equation describing it, we can understand it if we know "the principles involved and something of the order of their importance"[62]. In following his insight, we postulate that for the property of heart function and development the leading order of importance belongs to the bundled helical arrangement of muscle fibers. We follow this road map and utilize modeling tools to approach this question.

3.1.2 Modeling

Biological pumping organs are complicated multi-scale systems, and great efforts are directed at their computational modeling [41–43, 45, 51]. Despite the very significant resources applied and the impressive results achieved, it is currently an insurmountable challenge to computationally represent all the scales and aspects of these systems in their entirety. There exist neither a powerful enough computer, nor a sufficient understanding of the chemistry and control of muscle fibers to model complicated structure encompassing all the scales from the actin filaments up to the organ as a whole. At the same time, there is a great demand especially from the medical community, for models that trade the microscopic details for predictive power [55, 59]. In our opinion, and according to the experience of the engineering field, models should be based on the insight into the biologically dominant features of the system. In such a situation it would benefit us to be able to model the action of muscle without its intricate details. While the popular cardiac models are based on the fact that the fibers inside the heart are helical [20], the notion that they bundle into a single band that is arranged into a double helix [21], has never been properly simulated. It is easy to fathom that such helical structures could be used to optimize the functional properties of the organ, such as for example pumping. We model these macrostructures as applied to a problem of pumping. Meanwhile, knowing that a lot of times band like muscle fiber structures are results of self-assembly, we watch for characteristics that would be responsible for pushing the development of the tubular heart into the double helical arrangement. In that we take advantage of how nature uses these larger scale geometries and intricate dynamics to create wonderfully efficient mechanisms.

Here we present two simple models of biological pumps, for an embryonic fish and adult human hearts. We also consider different possibilities of contracting the muscles that operate these pumps.

3.2 Methods

3.2.1 Geometry of the ribbon models

3.2.1.1 Embryonic tube heart

An embryonic heart is shaped like a tube, which is one of the simplest chambers we can enclose with a band of fibers. The fibers can be arranged circumferentially or longitudinally, or they could form a spiral wound about the tube. Mathematically, such bands can be easily described by a set of parametric equations, which we omit for the sake of brevity [58]. Using these equations we can vary the different parameters of the spiral and tube: pitch (fiber) angle, number of turns, tube radius, tube length, fiber length, cylinder volume, width and thickness of the spiral band. The spirals with varying pitch angles are shown in figure 3.3. However, these parameters are not independent.

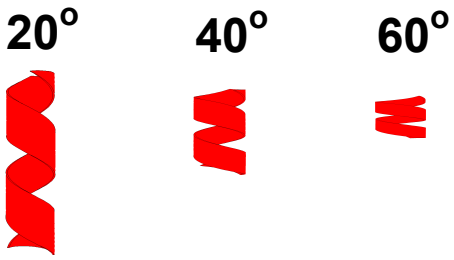

Figure 3.3: Images of the spiral muscle band models for the embryonic heart. The numbers indicate the pitch (fiber) angle: 20°, 40° and 60° are shown. For all three spirals shown here the radius of the tube is constant. The length of the band is also constant, and as a result the length of the tube varies with the pitch angle. The width of the band is taken to be half of the value that would have fully covering the surface of the tube, and as a result the width varies with the pitch angle.

3.2.1.2 Adult heart

A more complicated structure that also involves helical muscle fibers is the human adult heart. There is histological evidence that the fibers are arranged in a spiral band, as shown by Torrent-Guasp, who postulated that the heart muscle is a single band that starts from the pulmonary aorta, hugs the right ventricle, winds down to the apex, as the descending segment, and then spirals up to the aortic valve as the ascending segment. It is, of course, more complicated in terms of mathematical presentation than a simple spiral, but the parametric equations can still be written down using the same mathematical tools [58]. The resulting structure can be seen in figure 3.4A,

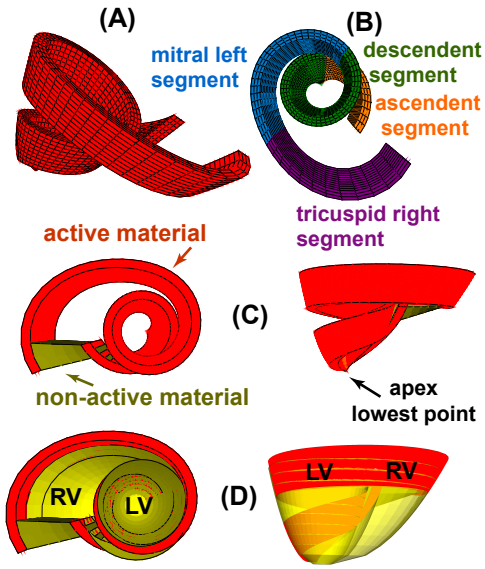

Figure 3.4: Images of the double helical band model of the adult heart. The initial band shape and fitted volume shown from different points of view. (A) The double helical band; (B) the same band color-coded corresponding to physiological segments. (C) The same band in different orientation, with labeled active and non-active material, as well as the apex of the heart. (D) The fitted volumes for left ventricles (LV) and right ventricle (RV) are labeled on these pictures.

with the physiological sections referenced in 3.4B. Figure 3.4D shows how such a relatively simple band structure could be filled out to form a full two ventricle heart.

3.2.2 Choosing the Geometrical Parameters

In both geometrical models, of tube-like embryonic heart and a double helical adult heart, there is a range of parameters that can be varied. We base the choice of parameters on physiological observations, the goals of the simulations, and computational needs.

3.2.2.1 Embryonic tube heart

Number of turns: In order for the spiral wound about a tube to be deformable into a double helix it needs to make two complete rotations. Thus the spiral makes two full turns. In our model we specify it to go around another quarter of a turn, so that the boundaries do not impact the main body of the spiral.

Pitch angle: It is not possible to extract the fiber angle (fiber angle) from the images of the embryonic heart. We therefore wanted the ability to vary the fiber angle. In the experiments the angle is varied between 5° and 80°.

Radius of the tube: In the embryonic heart model the radius of the tube is known, but it is

unclear how far up the tube the spiral fibers extend. Thus, we chose to keep the radius of the tube constant, namely 0.25 cm.

Length of the tube: Once both the number of turns of the spiral and the pitch angle are specified, the length of the tube is mathematically determined.

Fiber length: Once the above parameters are chosen the fiber length is determined.

Band width: The choice of the above parameters also defines the width of the band necessary to cover the whole surface of the tube. We chose for the width of the band to be limited to half of what would cover the tube, to insure that the material did not impinge on itself during twisting.

Band thickness: The thickness of the band is constant and small compared to the width (approximately 1/5 of the width).

3.2.2.2 Adult heart

Number of turns: This parameter is dictated to be two turns by the model design.

Fiber angle: Unlike the pitch angle of the simple spiral, the fiber angle is not constant in the double helical arrangement. We took the information from the histological studies done by Torrent-Guasp. As a result, the math description, although more cumbersome than in the case of the tube, is still known.

Long axis dimension: The long axis dimension is taken to be the same as in the normal adult heart, about 7 cm.

Basal radius: Again the basal radius is taken to be the same as in the adult heart, about 3.5 cm.

Right heart size: The parameter controlling the size of the right heart, was estimated so that the fitted right ventricle volume would correspond to the volume in a normal adult heart (about 130 mL).

Band width: To ease computation the band width is assumed to be a constant. The width is chosen such that the bottom of the mitral left segment does not impinge on the top of the descending segment ($w \approx 2.5$ cm).

Band thickness: The thickness of the band is constant and small compared to the width ($t \approx 0.5$ cm).

3.2.3 Material properties

The properties of the macrostructures of the organ's muscle are inevitably dictated by the muscles building blocks. The muscle fibers contract along the length of the fiber, thus the muscle band which consists of a group of parallel muscle fibers will contract in the same direction. The fibers cannot contract much over 15% [16], and thus the band will not exceed this maximum shortening ratio at any point along its length. While it is shortening in the fiber direction the band will expand in the other two to conserve volume. The band can shorten as a whole, or parts of it can contract independently of each other. That means that the cells can act separately along the length of the band, the fibers in the width of the band can also contract at different times from each other. For simplicity, we assume a linear elastic response while the material is not excited. The material is incompressible, so the maximal computationally possible Poisson ratio is chosen, $\nu = 0.48$ (an ideal incompressible material has $\nu = 0.5$). The choice of the Young's modulus will be discussed in section 3.2.5.

As regards to the structure of the adult heart it was necessary to hold it together with a non-active material shown in figure 3.4C. The non-active material was chosen to be four times softer then the active material, i.e., the Young's modulus of the non-active material is one fourth of the Young's modulus of the active material.

3.2.4 Boundary conditions

Unlike inside a body, our models are not part of a whole organism. It is, therefore, necessary for us to fix them in space. To do that we need to constrain at least three degrees of freedom, i.e., the x-direction, y-direction, and z-direction.

3.2.4.1 Embryonic tube heart

We found that the most meaningful results are obtained by fixing both ends of the tube. This allows us to consistently look at twisting and pumping in a range of different contraction schemes. If only one end of the tube is fixed, the other flaps about, which makes it hard to determine if there is any twist present.

3.2.4.2 Adult heart

In order to easily compare the dynamics of our model to the heart's dynamics, we wanted to fix the model in space in the same manner as the heart. In the body, the heart's apex does not move up or down, while the top of the heart does not rotate. The band structure is fixed in the horizontal plane by the non-active material, in the same manner as the heart is constrained by the vessels.

The lowest point of the double helix is assumed to be the apex, and is constrained in the vertical direction (figure 3.4C).

3.2.5 Excitation schemes

The simplest dynamic scheme is to excite all the cells at the same time and have the whole band contracting in sync. In this case the only periodicity is in time, so we call this a "uniform contraction."

The other choice is to excite a spatio-temporal wave contraction in the bands. Of course, in creating spatial waves, there are a lot of degrees of freedom. We can change the duration of the contraction, the length of the wave, the origin point of contraction, etc. Here we consider two examples of one dimensional spatial-wave excitation.

To ease the explanation let us label one end of the band α and the other β. A one dimensional contraction wave would then be described as originating from end α of the band and traveling to end β. This means that all the elements in width and thickness, the ones at the same centerline natural coordinate, will contract and relax together.

For ease of comparison to the uniform contraction, where all the elements are contracted in sync, we create a wave that has the contraction front traveling from end α of the band to end β. Once the contraction front reaches the β end of the band, the relaxation front starts from the original α end. This means that there is one instance of time where the whole band is contracted. We call this the "long wave contraction."

We also run simulations where the wave is shorter and the relaxation front starts before the contraction front reaches the β end. We called such a wave a "medium wave contraction."

For all the different types of contractions the maximal amplitude of enforced stress was adjusted such that at the given Young's modulus of the active material, the resulting strain does not exceed physiological constraints discussed in section 3.2.3.

3.2.6 Computational methods

To enable spatio-temporal excitation it is necessary to allow different sections of the bands to contract independently. This creates a complex coupling between local small deformations and huge global shape responses, making it a challenging modeling problem. Another difficulty is that we are considering three dimensional geometries. To combat these problems, we utilize the idea of finite elements. It is possible, with small quadrilateral elements to build very complicated shapes. The finite element method also breaks down a complicated problem of the dynamics of a complicated system in response to deformation into a set of manageable equations. Since this set is very large, it behooves us to use the computing power available to solve it. We therefore, model these bands

using a finite element package, ABAQUS, designed to handle such problems. In the finite element code we use ABAQUS built in tools to independently "excite" each node, and when the nodes of an element are "excited," the element contracts in the direction of the longitudinal fiber direction.

3.2.7 Data Analysis

Fortran and Matlab codes are used to extract and analyze the data from the simulations. For the purpose of this analysis we extract the position of each node from the simulation. Using this information we calculate the volume. In case of the embryonic one chamber tube model, the volume is approximated as a cylinder. During the deformation the diameter of the cylinder may vary as a function of the long axis. For the double helical, two pumping chamber model of the adult heart, the left ventricle volume is approximated as non-axisymmetric paraboloid. The shape of this paraboloid varies in the course of the beat.

In these simulations we do not model fluid. That means that it is unnecessary for us to model valves. Unless an actual pump has valves, it is very ineffectual. Indeed in the absence of valves most of the blood pumped during a contraction will flow back during relaxation. We thus assume that the valves are present. This assumption implies that if the volume of the chamber is increased, there will be blood sucked into the pump from the inlet. When the volume of the chamber is decreased, the blood is forced out through the outlet. Therefore, we can simply keep track of the volume that would fit inside the spiral to calculate the effectiveness of the pump.

To create a meter stick for our computational experiment we calculate the ejection fraction, for each system as it deforms with time:

$$\mathrm{EF(t)} = \frac{\mathrm{V_{max}} - \mathrm{V(t)}}{\mathrm{V_{max}}} \quad \text{and} \quad \mathrm{EF_{max}} = \frac{\mathrm{V_{max}} - \mathrm{V_{min}}}{\mathrm{V_{max}}}, \tag{3.1}$$

where, $V(t)$,V_{max} and V_{min} are the volume at time t, maximum volume and minimum volume of the chamber, respectively. This is the same formula that is used to find the ejection fraction in physiology for adult hearts, where $V_{max} = V_{end\ diasotolic}$ and $V_{min} = V_{end\ systolic}$.

To judge the dynamics of the simulations we use the visualization techniques available in a specialized software – ABAQUS CAE. For the tube model we overlay a wire-frame of the initial configuration on the transformed configuration. This way it is possible to directly compare the original and deformed spiral shape. For the double helix adult heart model, we create a piece of very soft material that is fixed to the side of the simulated left ventricle. To make sure that this indicator does not impact the dynamics, it's made from a material that is two orders of magnitude softer than the material of the band (i.e., the Young's modulus of the elastic indicator is one hundredth of the Young's modulus of the active material). Since the elastic indicator is attached along the length of the left ventricle, it will indicate the amount of twist. If the elastic indicator deforms symmetrically

there is no twist. However, if it deforms sideways, there has to be a twist present.

3.3 Results

We originally hypothesized that the cause of twisting in the embryonic tube heart is the response of the helical structure of the muscle fibers to muscle contractions. To test our hypothesis we created a spiral band wound about a tube. As our first simulation we induced a uniform periodic contraction. This means that at each heart beat the spiral was uniformly contracted and then released.

3.3.1 No twist in a uniformly contracted spiral band

The fiber angle did not have appreciable impact on the dynamics, throughout the range of meaningful values of 5° to 80°. Figure 3.5A shows a series of snapshots of the simulation for a representative fiber angle of 50°. Initially the muscle bands are relaxed (red), then they are gradually contracted, until the elements reach the maximum allowable strain (blue), and then they are relaxed again. The outline of the original configuration is overlayed on each spiral band. The radius of the band at the maximum contraction ($t = 0.4s - 0.6s$) is smaller than the original radius. The snapshots of the simulation show how the spiral smoothly contracts about the central axis and then gradually releases. No perceptible twist is apparent in these images. Thus the forces present are incapable of inducing a twist in the structure. We could have been disappointed by this result, if we did not have an insight from modeling the adult heart.

3.3.2 Back to the future: Adult heart model

To answer this quandary we turn forward, in ontogeny time, to the adult heart. In the adult heart the contraction of the muscle fibers yields an intricate dynamics, the heart twists at each beat [27–29]. If we understand the origin of this twist, we can hope to understand the twist in the embryonic heart. We can draw conclusions about the dynamics of the embryonic heart from our findings on the adult heart, because in both cases any movements are caused by the contraction of the muscle fibers.

In the adult heart the contraction is induced by the Purkinje network. This nerve network does not excite the whole myocardium at once. It is, therefore, unlikely that the myocardium contracts all at once. As a result, the adult heart is subject to spatial-wave contractions instead of a uniform contraction.

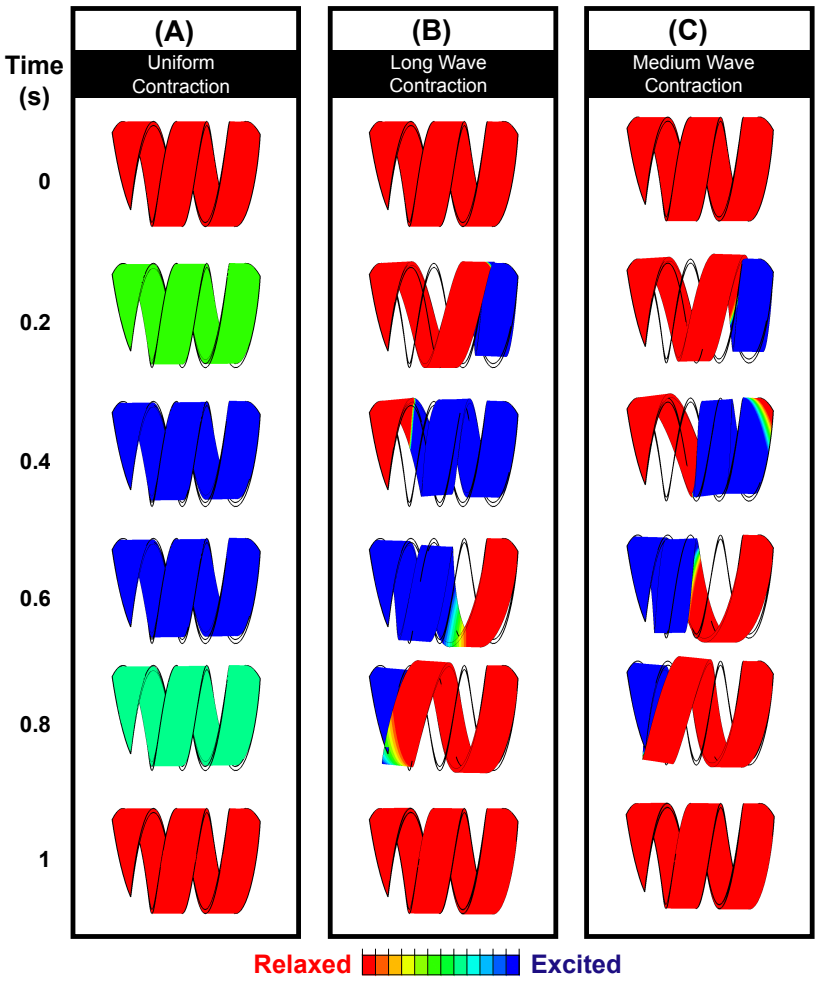

Figure 3.5: Snapshots of the ABAQUS simulations at different time steps for the embryonic heart spiral model with a 50° pitch (fiber) angle. The left column indicates the time in seconds. Each snapshot shows the current configuration of the spiral. The colors indicate the level of excitation as shown in the panel at the bottom, blue-fully excited, red-relaxed. Each simulation starts at the relaxed state ($t = 0s$), goes through the contraction scheme and relaxation scheme, and ends back in the fully relaxed state ($t = 1s$). For comparison purposes, an outline of the initial shape of the spiral is overlayed on each picture as a thick black line. (A) Uniform contraction. Here the spiral smoothly contracts during $t = 0s - 0.4s$, and smoothly relaxes during $t = 0.6s - 1s$. The radius is smallest when the band is fully contracted $t = 0.4s - 0.6s$. There is no change if pitch angle as seen by comparing the current configuration with the outline of the initial shape. Thus, there is not twist in this simulation. (B) Long wave contraction. The contraction wave front starts at the right end ($t = 0.2s,\ 0.4s$) and travels through the band to the left end. The band is fully contracted at approximately $t = 0.5s$. The relaxation front starts at the left end of the band ($t = 0.6s,\ 0.8s$) and travels to the other end. The radius is reduced unsymmetrically along the length of the tube ($t = 0.4s - 0.6s$). The pitch angle is changed drastically as seen from comparing the current band to the outline of the initial configuration ($t = 0.2s - 0.8s$). This indicates that there is a twist in the tube. (C) Medium Wave contraction. The contraction wave front starts at the right end ($t = 0.2s,\ 0.4s$) and travels through the band to the left end. The band is never fully contracted. The relaxation front starts at the left end of the band ($t = 0.6s,\ 0.8s$) and travels to the other end. The radius is reduced unsymmetrically along the length of the tube ($t = 0.4s - 0.6s$). The pitch angle is changed drastically as seen from comparing the current band to the outline of the initial configuration ($t = 0.2s - 0.8s$). This indicates that there is a twist in the tube.

3.3.2.1 Simulations of the Adult heart

The idea of spatial-wave contractions is rarely considered in cardiac modeling. This is mostly due to the fact that the majority of cardiac models are so complex that it is a challenge to test such cases. For our simplified model we were able to test such spatial-contraction patterns. Figure 3.6 shows time snapshots of simulations with different excitation schemes. In each of the series of pictures the level of excitation is color coded, with red as relaxed, and blue as fully excited. The excitation wave front starts at one end of the band and travels to the other. It is followed by a relaxation front moving in the same direction. We can vary the time between the contraction and relaxation fronts as one of the variables of the system. Thus, one of the possible wave-like contractions will have the whole band fully contracted at some point in time (figure 3.6B). However, it is also possible that the spatial-contraction wave never contracts the band fully (figure 3.6C). One may worry that the wave contraction would negatively impact the pumping ability.

3.3.2.2 How uniform vs. spatial-wave contractions affect pumping ability: Adult heart model

To insure that pumping efficiency was not negatively affected we tested the double helix model of the adult heart under both a uniform contraction and a spatial-wave contraction. The results of these tests were judged by calculating the left ventricular ejection fraction. The use of this particular criteria is justified by the fact that a large amount of physiological data is available for the left ventricular ejection fraction. To calculate the ejection fraction, we approximated the left ventricle as a paraboloid and calculated the volume at each time step. The ejection fraction is then simply given by equation 3.1.

The results for our simplified model easily match the physiological data of maximal ejection fraction. The values in table 3.3.2.2 show no drawback to having a spatial-wave contraction, as compared to a uniform contraction.

		Contraction Type		
	Physiological	Uniform	Medium wave	Long wave
Maximal EF	50%-60%	54%	54%	53%

Table 3.1: The ejection fraction values for double helical pumps under different excitation patterns

3.3.2.3 Different dynamics caused by spatial-waves

What is more fascinating is that the different contraction schemes produce different dynamics of the structure. Figure 3.6 shows the snapshots of the three simulations side by side. The twist is easily visualized by keeping track of the elastic parabolic indicator we fixed at the side of the structure's left

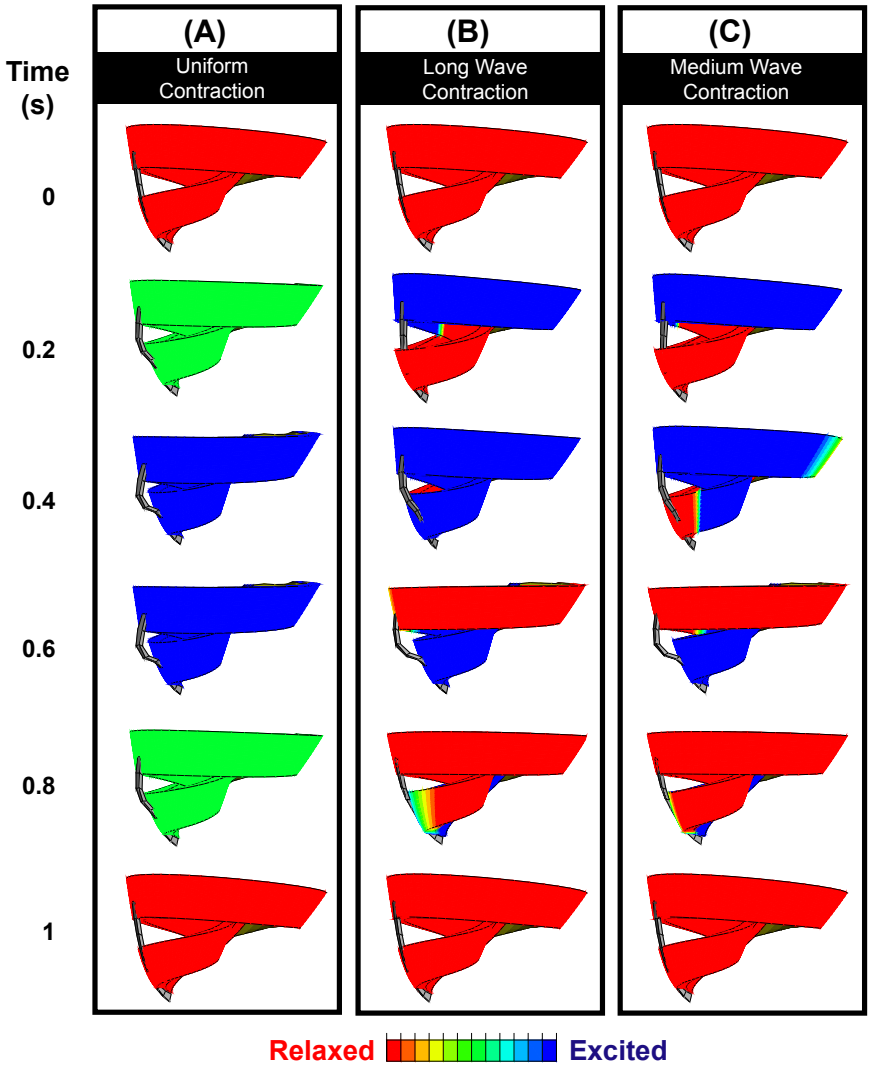

Figure 3.6: Snapshots of the ABAQUS simulations at different time steps for the adult heart double helix model. The left column indicates the time in seconds. Each snapshot shows the current configuration of the double helix. The colors indicate the level of excitation as shown in the panel at the bottom, blue-fully excited, red-relaxed. Each simulation starts at the relaxed state ($t = 0s$), goes through the contraction scheme and relaxation scheme, and ends back in the fully relaxed state ($t = 1s$). From this point of view, the volume reduction can be seen in how the top and bottom parts of the band come together during the contraction. A soft elastic material piece, indicated in dark gray, is fixed to the side of the left ventricle. (A) Uniform contraction. Here the double helix smoothly contracts during $t = 0s - 0.4s$, and smoothly relaxes during $t = 0.6s - 1s$. There is no twist of the left ventricle as indicated by ends of the gray material piece having a symmetric vertical position on the helical band. (B) Long wave contraction. The contraction wave front starts at right heart end ($t = 0.2s,\ 0.4s$) and travels through the band. The band is fully contracted at approximately $t = 0.5s$. The relaxation front starts at the right ventricle end of the band ($t = 0.6s,\ 0.8s$) and travels to the other end. The gray elastic material does not deform symmetrically ($t = 0.4s - 0.6s$). This indicates that there is a twist of the left ventricle. (C) Medium Wave contraction. The contraction wave front starts at right heart end ($t = 0.2s,\ 0.4s$) and travels through the band. The band is never fully contracted. The relaxation front starts at the right ventricle end of the band ($t = 0.6s,\ 0.8s$) and travels to the other end. The gray elastic material does not deform symmetrically ($t = 0.4s - 0.6s$). This indicates that there is a twist of the left ventricle.

ventricle. The piece of elastic material deforms in a the same radial plane for the uniform excitation scheme (figure 3.6A, $t = 0.2s - 0.8s$). For the both the long and medium wave contraction, at some time step the indicator deforms out of the radial plane (figure 3.6B and 3.6C $t = 0.4s - 0.6s$). This means that the double helical structure twists in cases where the excitation is wave-like and does not in the case of a uniform excitation. This gives us a hint that maybe a wave type excitation in a tubular model could also be related to the twist.

3.3.3 Forward to the Past: Embryonic heart model

We tested a spatial-wave contraction scheme in the spiral wound about a tube. Figures 3.5B and 3.5C show the time snapshots in which the contraction, represented in blue, starts at one end of the spiral and travels to the other end. The relaxation front, in red, follows the same pattern. As in the adult heart, the time between the excitation and relaxation front can be varied. In the uniform contraction scheme the whole spiral is contracted at once, which is not necessarily true for a spatial-wave contraction. The whole structure will be contracted, only if the two fronts are separated from each other by at least the length of the spiral.

3.3.3.1 How uniform vs. spatial-wave contractions affect pumping ability: Embryonic heart model

To insure that the wave-form contraction does not affect pumping we track the volume of the tube during the course of the beat.

Looking at the snapshots of the uniformly contracting tube simulation, one would suspect that the volume should change just as smoothly as the contraction (figure 3.5A). Indeed that is the case as seen in the figure 3.7.

As a matter of principle, it is possible for the spatial-wave contraction to affect pumping beneficially. Indeed, the spatial-wave contraction can induces not only simple shrinking, but also suction. In the plot of a representative fiber angle spiral undergoing a wave contraction the volume increases, then sharply decreases (figure 3.7A). This means that initially more fluid is sucked in and then a larger amount is ejected – larger than would otherwise be possible. The subsequent increase in volume would not produce back flow because of the valves. In the snapshots in the figures 3.5B and 3.5C it is possible to see qualitatively the cause of this suction. In the spatial-wave contraction, the part of the spiral that is contracting pulls on the piece that is still relaxed. In coming to mechanical equilibrium, part of the helix opens up, to reduce the stress on the band. So is this suction effect sufficiently beneficial to offset the fact that the whole band is not contracted at the same time?

For each contraction scheme we compared the maximal ejection fraction at different fiber angles. We use equations 3.1 to calculate the ejection fraction of these pumping tubes. Table 3.3.3.1 shows

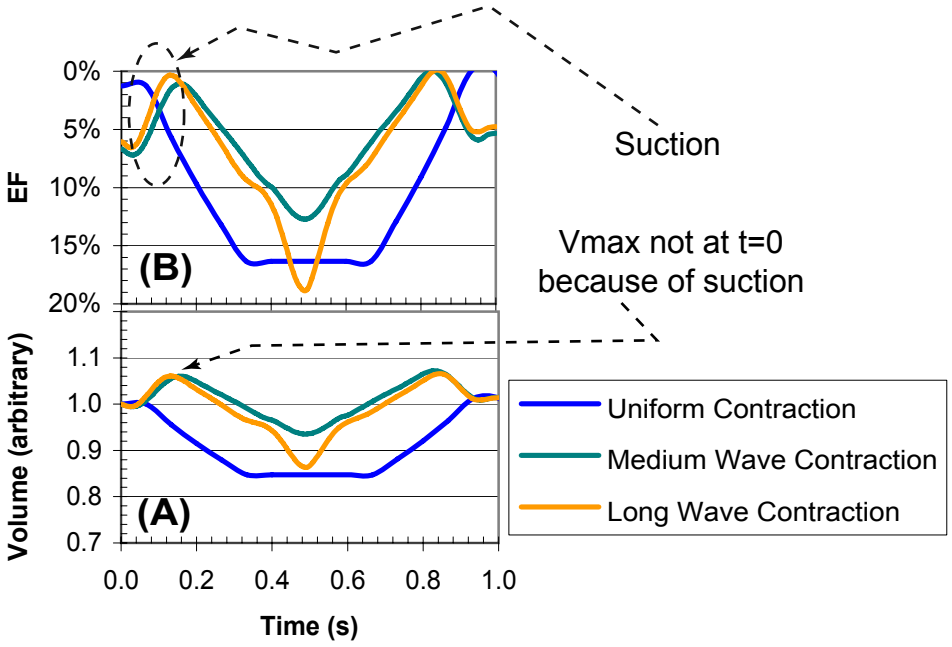

Figure 3.7: (A): Plot of normalized volume of the tube chamber vs. time. In case of wave-type contractions, the volume initially increases ($t = 0.04s - 0.15s$), because of suction. The volume is normalized over the initial value, and as a result the maximum volume in the case of wave contractions is at approximately $t = 0.15s$, as indicated by the arrow. (B): Plot of ejection fraction vs. time. The ejection fraction of the long wave contraction is greater than that of the uniform contraction, because of suction. The period of suction is circled with a dotted line.

the ejection fraction for spirals with different fiber angles undergoing different contraction schemes.

Even a spatial-wave contraction that does not contract the whole spiral is not a significant detriment to the pumping efficiency of the tube. Indeed, at some fiber angles a spatial-contraction scheme is beneficial to the effective pumping. This shows that the spatial-wave does not negatively impact the pumping efficiency. So did it produce twist?

3.3.4 Evidence of twisting in a spiral undergoing a spatial-wave contraction

The snapshots in figure 3.5B and 3.5C qualitatively show that there is an asymmetry in how the spiral deforms. Unlike the deformations in response to a uniform excitation, for both wave excitation patterns the deformed shape is significantly offset from the original outline. Indeed the same mechanism that causes suction produces this radical deformation. In a tube, this deformation would correspond to a twist, to accommodate the change in pitch angle of parts of the spiral.

This begs the question: Maybe the characteristic of leading importance is the wave like contrac-

	Contraction Type		
Pitch Angle	Uniform	Medium Wave	Long Wave
5	24%	18%	18%
10	23%	19%	24%
20	9%	7%	10%
30	11%	7%	9%
40	13%	7%	11%
50	17%	13%	19%
60	21%	21%	29%
70	23%	30%	36%
80	20%	34%	38%

Table 3.2: The ejection fraction values for tubular pumps with different pitch (fiber) angles, under different excitation patterns

tion, and not the helical shape as we originally claimed? If we had induced the propagating wave contraction in a simple tube with either longitudinal fibers or circumferential fibers the forces would have been in the axial or circumferential directions, respectively. As a result, the pumping efficiency would be reduced, since there would be no suction effect. In the longitudinal fiber case the length of the tube would decrease, without opening up any part of the tube. In the radial fiber case, the radius of the tube would simply decrease unsymmetrically, but no twist would occur. Therefore, this model shows that only the combination of the helical structure and the spatial-wave type contraction scheme produces the twist necessary for further development. And this is the main result of this study.

3.4 Conclusions

As Martin Kemp observed in his treatise on "spirals of life" [63], helical designs in living creatures are generally appreciated for their static structure, rather than the active functional benefits they bring. There are many examples in nature where there is a helical muscle structure, ranging from worms to embryonic fish hearts [5, 10, 57]. We have shown here that the helical structure cannot be the sole cause of the mechanical twist necessary for development. If the contraction of the spiral is smooth and symmetrical it cannot lead to twist.

In the adult heart the twisting dynamics are well documented. But, it is also well known that the adult heart is excited in a complicated pattern. By modeling spatio-temporal excitation waves and simple temporal excitation in the adult heart model we show that the twist is only possible if the excitation is in the form of spatial waves. Additionally, we have shown that no negative effects on pumping efficiency are brought about by wave-like contractions.

By applying this knowledge to the embryonic heart we were able to demonstrate twisting of the spiral structure. The spiral tube's pumping ability is also not impacted by switching from a uniform

excitation to a spatio-temporal excitation.

In light of these results we can form a better understanding of the development history of the heart. In the embryonic tube heart the fibers are organized helically. As it starts to beat the excitation pattern is not uniform, but is instead wave-like. The stress produced by the twisting of the the tube under these conditions forces the tube to bend. Thus, begins the road of phylogeny changing the simply spiraled muscle fibers into a double helix structure of the adult heart.